# HOG-Based Person Following and Autonomous Returning Using Generated Map by Mobile Robot Equipped with Camera and Laser Range Finder

Masashi Awai, Takahito Shimizu and Toru Kaneko

Department of Mechanical Engineering, Shizuoka University
3-5-1 Johoku, Naka-ku, Hamamatsu-shi, Shizuoka 432-8561, Japan
{f0130004, f0030029, tmtkane}@ipc.shizuoka.ac.jp

Atsushi Yamashita and Hajime Asama

Department of Precision Engineering, The University of Tokyo
7-3-1 Hongo, Bunkyo-ku, Tokyo 113-8656, Japan
{yamashita, asama}@robot.t.u-tokyo.ac.jp

**Abstract.** In this paper, we propose a mobile robot system which has functions of person following and autonomous returning. The robot realizes these functions by analyzing information obtained with camera and laser range finder. Person following is performed by using HOG features, color information, and shape of range data. Along with person following, a map of the ambient environment is generated from the range data. Autonomous returning to the starting point is performed by applying a potential method to the generated map. We verified the validity of the proposed method by experiment using a wheel mobile robot in an indoor environment.

**Keywords:** Mobile Robot, Laser Range Finder, Camera, Person Following

## 1 Introduction

In recent years, introduction of autonomous mobile robots to environments close to us is expected. Examples include shopping cart robots returning automatically to the shopping cart shed after shopping, and guide robots directing the way from the current location to the starting point in unknown environments. A robot which accomplishes these purposes needs functions of person following and autonomously returning to the starting point functions [1]-[3]. In this paper, we propose a mobile robot system that has functions of human following and returning to the starting point autonomously while avoiding obstacles.

The proposed mobile robot follows a person by using shape of range data, HOG (Histograms of Oriented Gradients) features, and color information, in parallel with generating a map by LRF data on the outward way from the starting point to the goal. On the return way, the mobile robot returns to the starting point autonomously while avoiding obstacles by using the generated map.

## 2 Outline

In this paper, we verify the validity of the system using the mobile robot equipped with the Laser Range Finder (LRF) and the camera. The mobile robot acquires two-dimensional (2-D) range data of 180 degrees forward by the LRF. The mobile robot also acquires the image in the front direction by the camera.

The operating environment of the mobile robot is a flat and static environment, and the mobile robot moves in 2-D space.

The mobile robot detects and follows a person by using the LRF and the camera when moving on the outward way. At the same time, the mobile robot generates a map with range data measured by the LRF.

The mobile robot generates a potential field from the generated map by an artificial potential method. Then, it moves on the return way along gradient directions of the generated potential field. At the same time, the mobile robot avoids obstacles not recorded in the map by reconstruction of the potential field.

## 3 Person Following on Outward Way

The mobile robot performs person following and map generation on the outward way. In this paper, the mobile robot follows the person by using person detection.

Person detection is performed by evaluating a value of person likelihood. The value of person likelihood is evaluated on the shape of range data and the HOG features in acquired images. However, this evaluation is ineffective to follow the person in environment where more than one person exist. Because, the shape of LRF data and HOG features are not specific to the person to be followed but common to all persons. Therefore, color information is added to the shape of range data and HOG features.

We use a particle filter for person following. In particle filter algorithm, a particle is assigned a weight at each particle position. However, calculation of weight at each particle position is computationally expensive. Thus, assigning the weight to the particle is performed as follows. First, the robot acquires range data (Fig. 1(a)). Next, values of person likelihood are evaluated only at the range data positions (Fig. 1(b), (c)). In the particle filter algorithm, particles near to range data positions are assigned a weight as evaluated values.

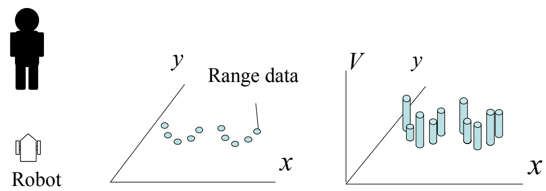


(a) Measurement. (b) Range data. (c) Evaluation.

Fig. 1. Data evaluation.

### 3.1 Evaluation on shape of range data

Evaluation on the shape of range data uses template matching proposed in [4].

The 2-D map image is generated from the range data measured at each angle for the template matching. In the 2-D map image, the region beyond the detected range is in black and the other region is in white. Fig. 3 shows leg template for matching in the 2-D map image.

While following the person, matching scores are obtained by performing the matching at each range data position in the 2-D map image. Matching score $R$ is obtained by SAD (Sum of Absolute Difference).

$$R = \sum_{j=0}^{M} \sum_{i=0}^{M} \left| I(i,j) - T(i,j) \right|, \tag{1}$$

where $T(i, j)$ is a pixel value on the template image ($M \times M$). $(i, j)$ is position on the image, and $I(i, j)$ is a pixel value on the 2-D map image.

Equation (2) shows person likelihood score $P_L(\theta)$ of the range data position whose angle is $\theta$.

$$P_L(\theta) = 1 - aR(\theta), \tag{2}$$

where $R(\theta)$ is a matching score of the range data position whose angle is $\theta$, and $a$ is a parameter for normalizing value of $R(\theta)$.

Finally, Equation (3) shows the evaluated value on shape of range data $V_L(\theta)$.

$$V_L(\theta) = \frac{P_L(\theta)}{\sum_{\theta=0}^{N} P_L(\theta)}, \tag{3}$$

where $N$ is number of range data.

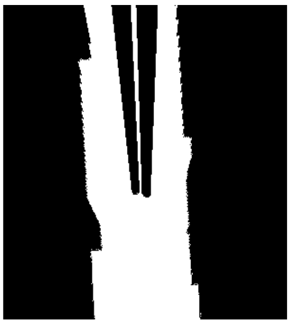

Fig. 2. Range data.

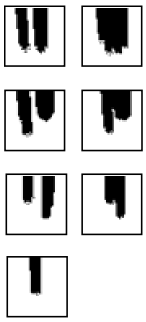

Fig. 3. Leg templates.

### 3.2 Evaluation on HOG features

Person detection in acquired images is performed by using the Real Adaboost algorithm with HOG features. The validity of HOG features for person detection is verified in [5].

For person detection on HOG features, image regions to perform person detection are selected in acquired image. By setting the size of person, the size and position of the image region are determined according to each range data position (angle and distance). Person likelihood score $P_H(\theta)$ is calculated by performing person detection on each selected image region in the acquired image while following the person.

$$P_H(\theta) = bH(\theta) + c, \tag{4}$$

where $H(\theta)$ is the final classifier value of Real Adaboost on the selected image region according to range data position whose angle is $\theta$. $b$ and $c$ are parameters for normalizing value of $H(\theta)$. Equation (5) shows the evaluated value on HOG features $V_H(\theta)$.

$$V_H(\theta) = \frac{P_H(\theta)}{\sum_{\theta=0}^{N} P_H(\theta)}, \tag{5}$$

### 3.3 Evaluation on color histogram

Detecting the person to be followed is performed by using color histogram. To be robust to the change in brightness, the color histogram of hue $h$ and saturation $s$ is made by using pixel values converted into HSV. The mobile robot acquires color information on the person who is to be followed by the mobile robot before the person following begins.

While the mobile robot follows the person, the color information is acquired from the image region which is selected according to each position of acquired range data. Then, the color histogram is made and the degree of similarity with the color histogram made before the person following begins is calculated.

The Bhattacharyya coefficient [6] is used for calculating the degree of similarity with the histograms. Equation (6) shows Bhattacharyya coefficient $L(\theta)$ of range data position whose angle is $\theta$.

$$L(\theta) = \sum_{h}^{h_n} \sum_{s}^{s_n} \sqrt{H_t(h,s) \times H(h,s,\theta)}, \tag{6}$$

where $H_t(h, s)$ is the frequency of each bin of the color histogram of the person that is acquired before the mobile robot begins person following. $H(h, s, \theta)$ is the frequency of each bin of the color histogram acquired in image for angular $\theta$ direction while the mobile robot follows the person. $h_n$ is the number of bins of hue $h$, and $s_n$ is the number of bins of saturation $s$

Finally, Equation (7) shows the evaluated value on color information $V_C(\theta)$.

$$V_C(\theta) = \frac{L(\theta)}{\sum_{\theta=0}^{N} L(\theta)}, \tag{7}$$

### 3.4 Integration of evaluated values

The integrated value of person likelihood $V(\theta)$ is determined by $V_L(\theta)$, $V_H(\theta)$ and $V_C(\theta)$.

$$V(\theta) = \alpha V_L(\theta) + \beta V_H(\theta) + (1-\alpha-\beta) V_C(\theta), \tag{8}$$

where α(≥0), β(≥0) are weight coefficients.

### 3.5 Tracking by particle filter

Person following is performed by using a particle filter with value of $V(\theta)$. Particle filter is performed as follows.

(i) Initial particles are distributed around the person with random noise

(ii) Particles are moved based on the system model given by Equation

$$\mathbf{x}_{t|t-1} = \mathbf{x}_{t-1} + \mathbf{v}_{t-1} T, \tag{9}$$

where $\mathbf{x}_t$ is position in time $t$, $\mathbf{v}_t$ is velocity in time $t$, and $T$ is updating cycle.

(iii) Each particle is assigned a weight as $V(\theta)$ of near range data position.

(iv) New particles are generated depending on the weight as resampling process.

First, process (i) is performed. Next, processes (ii), (iii) and (iv) are performed. After that, processes (ii), (iii) and (iv) are performed repeatedly.

## 4 Map Generation on Outward Way

The mobile robot generates the map of ambient environment while it moves on the outward way. The LRF is used to measure the ambient environment during the mobile robot movement, and the ambient environment map is generated by integrating each measurement data. Measurement data integration needs an accurate self-location estimation of the mobile robot. In this study, the estimation is made by dead reckoning. However, dead reckoning has a problem of error accumulation caused by wheel slipping. In order to decrease this error accumulation, the robot aligns each measurement data by the ICP algorithm [7].

Moving objects do not exist in the same place. Therefore, it is necessary to remove moving objects from the map. The mobile robot removes moving objects by a method in [8].

## 5 Motion on Return Way

The mobile robot moves on the return way according to the Laplace potential method [9]. The robot generates the potential field in the map obtained on the outward way. Then the robot moves on the return way along a gradient direction of the generated potential field.

For the robot to avoid obstacles not recorded in the map, the LRF measures an ambient environment while the robot moves on the return way and the robot reconstructs a potential field. This makes the movement of the robot safe on the return way.

# 6 Experiment

## 6.1 Experiment device

We used the mobile robot ”Pioneer3” of MobileRobots, Inc (Fig. 4). The robot has 2 drive wheels and 1 caster. Its maximum speed is 400mm/sec. It turns with the velocity differential of right and left wheels. The LRF is model LMS200-30106 by SICK. It is equipped at a height of 30cm above the ground. The sensing range is 180 degrees in one plane and the resolution is 0.5 degrees.

The camera is equipped at a height of 80cm above the ground. As the specs on computers, CPU is Intel Core 2Duo T9300 2.5GHz, and memory is 3.5GB.

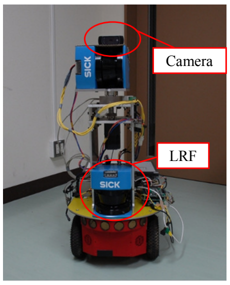


Fig. 4. Mobile robot.

Fig. 5. Environment.

## 6.2 Experiment environment

We conducted experiment in which the mobile robot follows a person to the goal and then returns to the starting point. Experiment environment is a corridor with a flat floor. Figure 5 shows the experiment environment. There are some pedestrians in experiment environment.

## 6.3 Experimental result

On the outward way, the mobile robot followed the person.

Figure 6 shows acquired data when the static obstacle is exists.

Figure 6(a) shows an image acquired with the camera while the robot followed the person. In Fig. 6(a), the person existing on the left is the person to be followed by the mobile robot.

Figure 6(b) shows a 2-D map image generated by range data acquired with the LRF. Particles are shown as red points in Fig. 6(b).

Figure 6(c) shows evaluation value on shape of range data $V_L(\theta)$. The horizontal axis in Fig. 6(c) indicates the view angle from the robot (the positive and negative values correspond to the right and left angle, respectively). In Fig. 6(c), it is shown that high values appear in the vicinity of the angle where the person and static obstacle exist.

Figure 6(d) and (e) show evaluation value on HOG features $V_H(\theta)$ and evaluation value on color information $V_C(\theta)$. It is shown that high values appear in the vicinity of the angle where the person exists.

Finally, Fig. 6(f) shows the integrated value of person likelihood $V(\theta)$. It is shown that the highest values appear in the vicinity of the angle where the person to be followed exists. It shows that using $V(\theta)$ is better than only using $V_L(\theta)$ for following person in this situation.

(a) Acquired image.

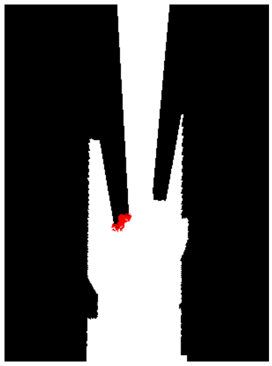

(b) Range data and particle

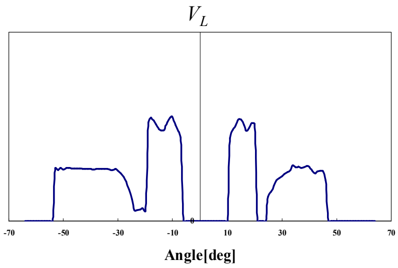


(c) Evalustion value of LRF $V_L(\theta)$.

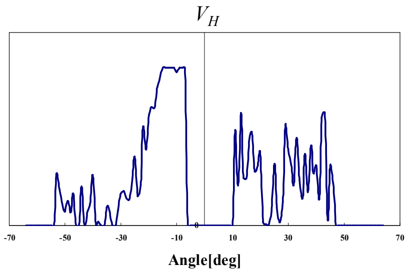


(d) Evalustion value of HOG $V_H(\theta)$.

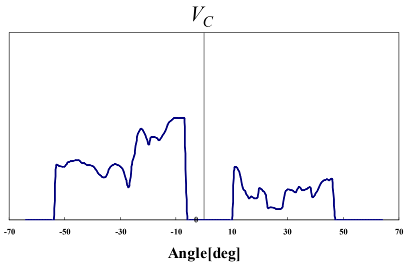


(e) Evalustion value of color $V_c\ (\theta)$.

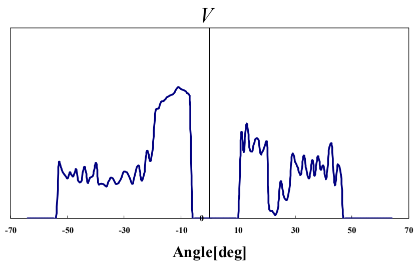


(f) Integrated evaluation value $V(\theta)$.

Fig. 6. Acquired data when the static obstacle is exists.

Figure 7 shows acquired data when the pedestrian is exists.

Figure 7(a) and (b) show acquired image and range data as with Fig. 6. The right person is the person who should be followed by the mobile robot.

Figure 7(c) and (d) show $V_L(\theta)$ and $V_H(\theta)$. High values appear in the vicinity of the angle where the persons exist.

Figure 7(e) shows $V_C(\theta)$. High values appear in the vicinity of the angle where the person to be followed exists.

Finally, Fig. 7(f) shows $V(\theta)$. High values appear in the vicinity of the angle where the person to be followed exists.

It is shown that using $V(\theta)$ is better than using $V_H(\theta)$, $V_L(\theta)$ for person following in this situation, and robust following can be performed even if high values in one evaluation appear in the vicinity of the angle where the person to be followed does not exist.

The mobile robot followed the person by using the particle filter in which particles are assigned the weight based on $V(\theta)$ in experimental environment.

(a) Acquired image.

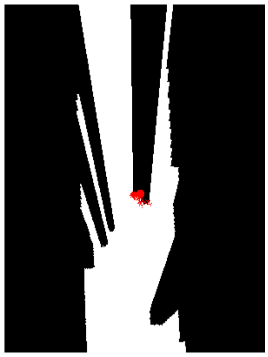

(b) Range data and particle

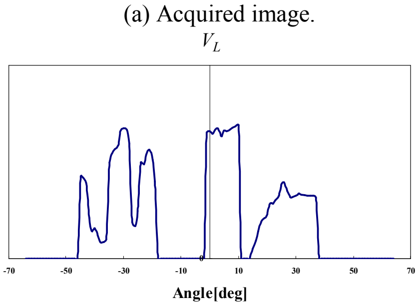


(c) Evalustion value of LRF $V_L(\theta)$.

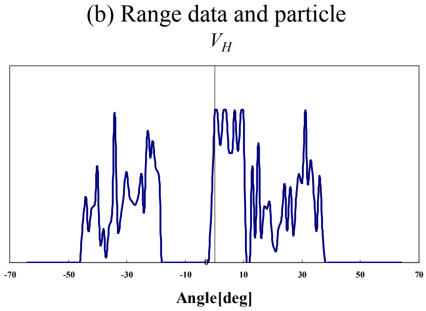


(d) Evalustion value of HOG $V_H(\theta)$.

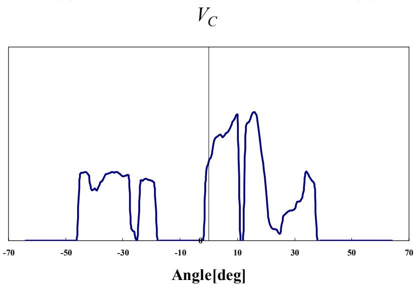


(e) Evalustion value of color $V_c(\theta)$.

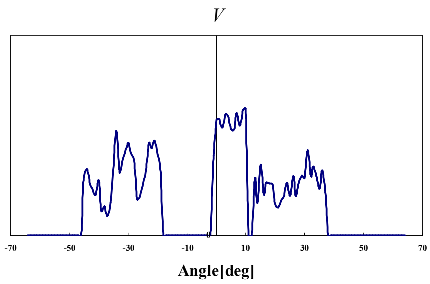


(f) Integrated evaluation value $V(\theta)$.

Fig. 7. Acquired data when the pedestrians exist.

Figure 8(a) shows the generated map and the robot trajectory on the outward way. It is shown that stationary object map was generated by moving object removal. The robot moved on the return way by using the map which had been generated on the outward way. On the return way, the new obstacle that did not exist on the outward way existed.

Figure 8(b) shows the trajectory of the robot on the return way. It is shown that the robot returned to the starting position while avoiding the new obstacle.

These results show that the mobile robot can detect and follow the person by the proposed method in the experimental environment and can return to the starting point while avoiding obstacles.

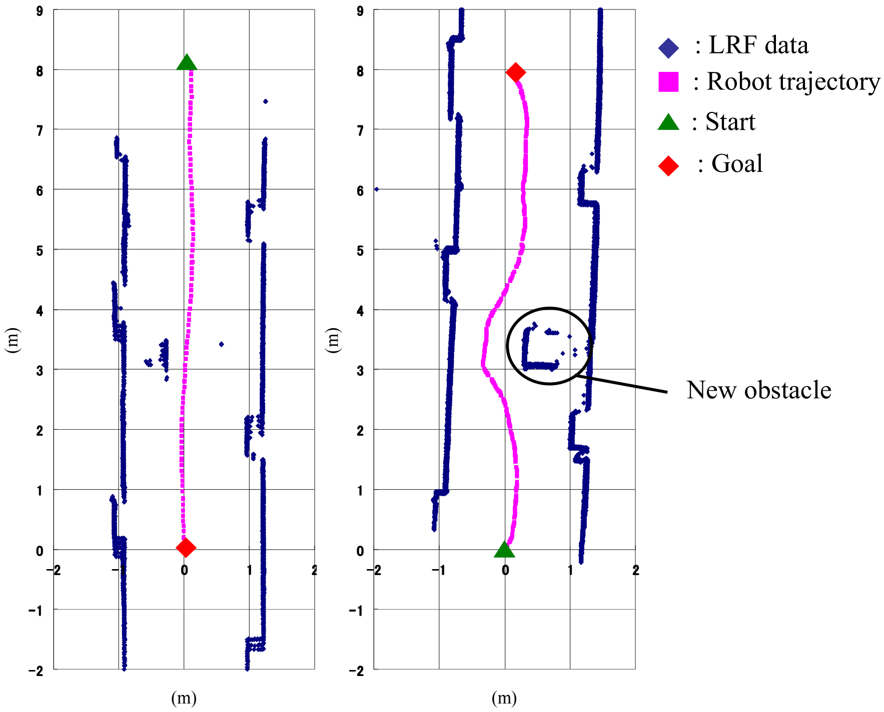


(a) Outward way (b) Return way

Fig. 8. Generated map and trajectory of mobile robot.

## 7 Conclusion

In this paper, we construct the mobile robot system that has functions of person following and returning to the starting point autonomously while avoiding obstacles.

Person following is achieved by using shape of range data, HOG features and color information. Map generation is achieved by the ICP algorithm and the moving object detection. The robot returns to the starting point according to the Laplace potential method with generated map, and a path of avoiding obstacle is generated by reconstructing a potential field.

## Acknowledgements

This work was in part supported by MEXT KAKENHI, Grant-in-Aid for Young Scientist (A), 22680017.

## References

1. M. Misawa, T. Yoshida and S. Yuta: "A Smart Handcart with Autonomous Returning Function", *Journal of Robotics Society of Japan*, Vol. 25, No. 8, pp. 1199-1206, 2007. (in Japanese)
2. T. Lixin and S. Yuta: "Mobile Robot Playback Navigation Based on Robot Pose Calculation Using Memorized Ominidirectional Images", *Journal of Robotics and Mechatronics*, Vol. 14, No. 4, pp. 366-374, 2002.
3. N. Tsuda, S. Harimoto, T. Saitoh and R. Konishi: "Mobile Robot with Following and Returning Mode", *Proceedigs of the 18th IEEE International Symposium on Robot and Human Interactive Communication* (RO-MAN2009), ThB1.3, pp. 933-938, 2009.
4. S. Okusako and S. Sakane: "Human Tracking with a Mobile Robot using a Laser Range-Finder", *Journal of Robotics Society of Japan*, Vol. 24, No. 5, pp. 605-613, 2006. (in Japanese)
5. N. Dalal and B. Triggs: "Histgrams of Oriented Gradients for Human Detection", *Proceedings of the 2005 IEEE Computer Society Conference on Computer Vision and Pattern Recognition*, pp.886–893, 2005.
6. T. Kailath: "The Divergence and Bhattacharyya Distance Measures in Signal Selection", *IEEE Transactions on Communication Technology*, Vol.COM-15, No.1, pp.52–60, 1967.
7. P. J. Besl and N. D. Mckay: "A Method for Registration of 3-D Shapes", *IEEE Transaction on Pattern Analysis and Machine Intelligence*, Vol.14, No.2, pp.239–256, 1992.
8. S. Iwashina, A. Yamashita and T. Kaneko: "3-D Map Building in Dynamic Environments by a Mobile Robot Equipped with Two Laser Range Finders", *Proceedings of the 3rd Asia International Symposium on Mechatronics*, TP1-3(1), pp. 1-5, 2008.
9. K. Sato: "Deadlock-free Motion Planning Using the Laplace Potential Field", *Proceedings of the Joint International Conference on Mathematical Methods and Supercomputing in Nuclear Applications*, pp. 449-461, 1994.